JOURNAL OF CATALYSIS 58, 348–360 (1979)

Mössbauer Investigation of Supported Fe and FeNi Catalysts

II. Carbides Formed by Fischer–Tropsch Synthesis

G. B. RAUPP[1] AND W. N. DELGASS

School of Chemical Engineering, Purdue University, West Lafayette, Indiana 47907

Received July 13, 1978; revised January 12, 1979

Mössbauer characterization of iron catalysts following Fischer–Tropsch reaction at 523°K reveals significant differences in carbide phases formed depending on particle, support, and alloying with Ni. Small iron particles on silica favor formation of the unstable ϵ' and ϵ carbides. Large iron particles on silica and small particles on magnesia form χ carbide as is normal for bulk unpromoted iron. Alloying iron with nickel in approximately equimolar amounts completely prevents formation of bulk carbides at our reaction conditions, but some evidence exists for formation of surface carbon. The complexity of the metastable $Fe/Fe_xC/C$ system is further exemplified in a series of spectra recorded at intermediate reaction times. These data demonstrate time dependency of carbide phases formed and dependence of the rate of carbide formation on average metal particle size.

INTRODUCTION

Research in the recently reawakened field of Fischer–Tropsch synthesis has concentrated on questions of specific reaction rates over different metals, the sequence of elementary steps describing the synthesis reactions, and the respective roles of promoters and alloying on catalyst activity and selectivity (*1–8*). For both fused (*9–12*) and supported (*13*) iron catalysts, these questions are complicated by the fact that metallic iron is transformed to iron carbide during reaction.

Literature data with regard to the reaction intermediate are divided between that supporting hydrogenation of some form of surface carbide and that supporting an oxygenated surface complex as the reactive precursor of hydrocarbon products (*14, 15*). Although the catalytic role of carbides remains a controversial subject, the fact that carbides have an important effect on the structure and the properties of the catalyst surface cannot be disputed. In this paper we report the effects of metal particle size, catalyst support, alloying, and time on stream on the nature of carbide formation in supported iron catalysts. The first paper in this series (*16*) presents a strong effect of dehydration on metal particle size and alloy formation. Part III deals with the catalytic significance of carbide formation during Fischer–Tropsch synthesis (*17*).

[1] Present address: Exxon Research & Engineering Company, Florham Park, N.J. 07932.

EXPERIMENTAL METHODS

Catalyst preparation. Iron and iron–nickel silica-supported catalysts were prepared from nickel and ferric nitrates and Cabosil EH5 ($\sim$400 m^2/g) by the incipient wetness method (*16*). Iron and iron–nickel on magnesia were prepared by hydrogen

0021-9517/79/090348-13$02.00/0

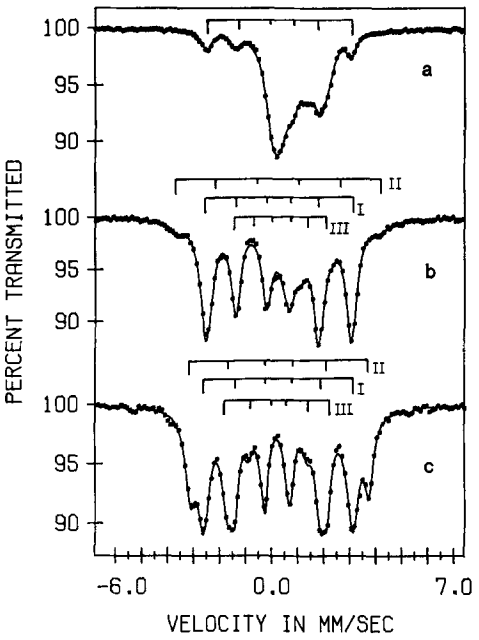

FIG. 1. Room temperature Mössbauer spectra of $10Fe/SiO_2$ catalysts carbided in 3.3 H_2/CO 6 hr at 523°K, then quenched in He. The stick diagrams indicate line positions and relative intensities of the ϵ' carbide (a) and the I, II, and III sites in ϵ carbide (b) and χ carbide (c). (a) 6.1-nm particles; (b) 7.4-nm particles; (c) 10.1-nm particles.

reduction of a magnesium hydroxycarbonate precursor prepared in a manner described by Boudart *et al.* (*18*). Magnesium carbonate basic powder [$4MgCO_3 \cdot Mg(OH)_2 \cdot 5H_2O$] obtained from Matheson, Coleman, and Bell and metal nitrate salts obtained from Mallinckrodt were used. This technique is based upon the overall ion-exchange reaction:

$$3Mg_{(s)}^{2+} + 2Fe_{(aq)}^{3+} \rightleftarrows 3Mg_{(aq)}^{2+} + 2Fe_{(s)}^{3+}$$

The solubility product of $Mg(OH)_2$ at 300°K is $K_{sp} = 5.6 \times 10^{-12}$; that of $Fe(OH)_3$ is $K_{sp} = 1.5 \times 10^{-36}$. Thus a driving force exists that constantly favors the dissociation of magnesium hydroxide in the presence of ferric ions. The ferric ions in turn precipitate from solution as $Fe(OH)_3$. A detailed study of the genesis of the catalyst from the precursor (*18, 19*) showed that the filtered, dried precursor maintains the platelike structure of magnesium hydroxycarbonate until hydrogen reduction decomposes these large particles to form smaller particles of magnesium oxide. The fairly uniformly distributed iron is simultaneously transformed to iron-rich clusters. All catalysts prepared in this manner are referred to as xFe/MgO or xFeyNi/MgO where x and y are wt% Fe and wt% Ni, respectively, on a dry, reduced basis. Similar notation is used for xFeyNi/SiO_2.

Catalyst characterization. Constant acceleration Mössbauer spectra were obtained with a conventional electromechanical spectrometer and *in situ* absorber cell described earlier (*16*). Isomer shifts are reported with respect to the NBS Fe foil used for calibration. Computer fitting of spectra was done with a variable metric minimization program as in (*16*). The lines drawn through the data points in the figures are the result of the computer fits. A General Electric XJD-5 X-ray diffractometer produced the X-ray diffraction patterns of the catalyst powders.

RESULTS AND DISCUSSION

Effect of Metal Particle Size

In this section we analyze Mössbauer data for various $10Fe/SiO_2$ catalysts after use in Fischer–Tropsch synthesis to show that smaller Fe particles tend to form the less stable ϵ' and ϵ carbide structures while large particles form the χ (Hägg) carbide. The strong influence of the SiO_2 support in this behavior is evident in the following section which shows that small iron particles on MgO favor the χ carbide.

Prior to reaction, the $10Fe/SiO_2$ catalysts were reduced in H_2 for ca. 8 hr at 675–750°K, cooled in H_2, analyzed by Mössbauer spectroscopy, and then brought to reaction temperature, 523°K, in flowing He. A premixed synthesis gas of composition 3.3 H_2/CO was flowed over the catalyst

TABLE 1

Spectral Parameters for Carbided 10Fe/SiO_2 Catalysts (Fig. 1)

Catalyst and pretreatment	Fe site	H (kOe)	IS (mm/sec)	Fractional spectral area[a]	d_{Ave}[b] (nm)	Percentage exposed (%)
(a) 10Fe/SiO_2 Air calcined 2 hr at 523°K	ϵ'	172.5	+0.28	1.00	6.1	14
(b) 10Fe/SiO_2	ϵ_I and ϵ'	172.6	+0.27	0.87	7.4	11
1% O_2/He	ϵ_{II}	243.0	+0.35	0.08		
calcined 12 hr at 648°K	ϵ_{III}	134.0	+0.25	0.05		
(c) 10Fe/SiO_2	χ_I	180.8	+0.24	0.52	10.1	8
1% O_2/He calcined 24 hr	χ_{II}	215.5	+0.30	0.30		
at 723°K	χ_{III}	116.1	+0.23	0.18		
	Fe^0	328.6	+0.02			

[a] Considering carbide phases only.

[b] Determined from X-ray line broadening of spent catalyst. No passivation was necessary since the carbide phases are stable in air at room temperature.

wafer at 100 cc/min for 6 hr. The catalyst was quenched from reaction conditions in 200 cc/min He. Figure 1 compares the room temperature Mössbauer spectra of the used catalysts as a function of average metal particle size; Table 1 summarizes corresponding spectral parameters along with particle size and dispersion (percentage exposed) data obtained from X-ray line broadening. In all cases, the average magnetic hyperfine field is substantially less than that of metallic iron (shown by the small peaks at ca. ±5 mm/sec in Fig. 1c) indicating the formation of Fe–C bonds characteristic of iron carbides.

For the smallest particles, Fig. 1a, most of the spectral area is in the form of a central asymmetric doublet attributed to unreduced ferrous ions. The absolute area under these peaks remained constant relative to that of the reduced samples; hence the reaction conditions do not enhance overall reduction of the catalyst. The computer fit hyperfine field (H) value near 172 kOe agrees within experimental error with the value of 170 kOe which previous workers (*20, 21*) estimate that hexagonal close-packed ϵ' carbide ($Fe_{2.2}C$) should have. In addition, a Mössbauer spectrum of ϵ' carbide has recently been reported by Amelse *et al.* (*13*) for a used 5 wt% Fe on silica catalyst. Their magnetic field value equal to 173 kOe and isomer shift (IS) of +0.25 mm/sec relative to α-iron agree quite well with the H and IS values for this catalyst. Further evidence supporting the assignment to ϵ' carbide was obtained with an estimation of the Curie temperature, T_c, of the ferromagnetic phase through temperature-dependent measurement of the internal magnetic field with Mössbauer spectroscopy. Table 2 summarizes literature data on bulk carbides and illustrates that, in principle, measurement of T_c can aid phase identification since the T_c differences between carbide phases are significant. For the 10Fe/SiO_2 catalyst corresponding to Fig. 1a, a definite, though reduced in splitting and intensity, hyperfine six-line pattern existed at 673°K. Thus this carbide phase can only be ϵ'. Attempts to determine an exact T_c failed because in the range 673–733°K the carbide decomposed to a combination of more stable carbides plus metallic iron. It should be noted that for other catalysts

TABLE 2

Bulk Iron Carbide Data

Carbide phase	Structure	T_c (°K)		H (kOe)	IS[a] (mm/sec)	Ref.
ϵ'-$Fe_{2.2}C$	Hexagonal close-packed	~720		173 ± 1	+0.25 ± 0.01	(*13*, *10*)
ϵ-Fe_2C	Transition from hcp to monoclinic	650	I	170 ± 3	+0.20 ± 0.05	(*20*)
			II	237 ± 3	+0.35	
			III	130 ± 6	+0.30	
χ-Fe_5C_2 (Hägg)	Monoclinic	525	I	184 ± 3	+0.30 ± 0.04	(*22*)
			II	222 ± 3	+0.35 ± 0.04	
			III	110 ± 6	+0.30 ± 0.08	
θ-Fe_3C	Orthorhombic	480	I	208 ± 7	+0.29 ± 0.02	(*22*)
			II[b]			

[a] Relative to α-Fe.

[b] I and II have fields degenerate within ±5 kOe.

with average metal particle size less than the 6-nm value for this catalyst, identical carbiding behavior was observed.

For a catalyst with somewhat larger average metal particle size (Fig. 1b the nature of the carbide phase is noticeably different. Small shoulders on the large outer peaks indicate that more than one type of magnetic iron exists. Since no carbide phases have only two iron sites, a computer fit with three overlapping sets of six lines was employed. Within each six-line set peak dips were constrained 3:2:1 and linewidths were constrained to be equal for companion peaks, i.e., peak 1 and peak 6, 2, and 5, and 3 and 4. The three resultant values for H of 172.6, 243.0, and 134.0 kOe, respectively, agree well with the literature values for ϵ carbide, which has a structure intermediate between hcp ϵ' and monoclinic χ carbide. The relative area ratios for the three sites reveal, however, that the spectral component corresponding to the Fe_I site is too intense compared to the theoretical ratio of $Fe_I:Fe_{II}:Fe_{III} = 4:1.6:1.0$, based on the known populations of the individual crystallographic sites in the ϵ carbide bulk lattice. This quantitative anomaly can be rationalized if the spectrum represents a combination of ϵ' and ϵ phases. Comparison of the local magnetic structures of ϵ', ϵ, and χ carbides shows that the ϵ phase contains elements of the other two. The most occupied magnetic site, Fe_I, in ϵ carbide is in fact the only position expected in ϵ' carbide. The two new positions Fe_{II} and Fe_{III}, also characteristic of the χ phase, arise from the rearrangement of iron and carbon atoms during the $\epsilon' \rightarrow \epsilon$ transition. For the catalyst in question, the Mössbauer spectrum shows (assuming equal recoil-free fractions) that the iron is two-thirds ϵ' carbide with the balance in the form of ϵ carbide. An X-ray diffraction scan detected only the three major reflections of ϵ carbide. A Mössbauer effect Curie temperature measurement, however, confirmed the presence of ϵ' carbide. Thus, it appears that the coexistence of the two phases is a result of an iron particle size distribution, with smaller particles (too small to be detected by XRD) favoring formation of ϵ' carbide and larger particles favoring the ϵ phase. The stability of these phases after very long reaction times has not yet been investigated.

As shown by Fig. 1c, further differences in carbide formation are observed when the average particle size of the reduced

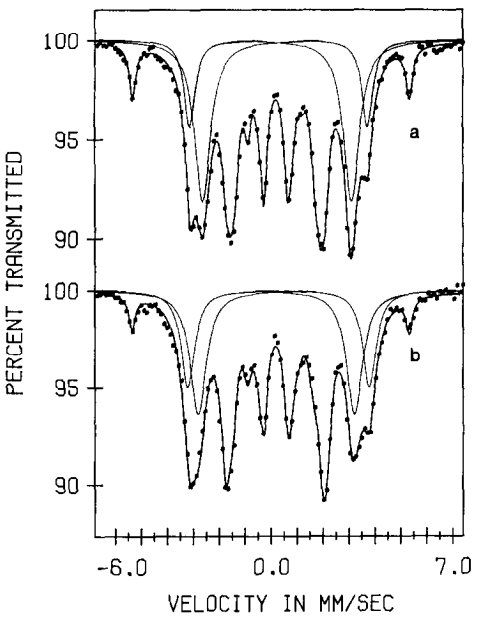

FIG. 2. Mössbauer spectra for partially carbided and partially rehydrogenated 10Fe/SiO_2. (a) 3.3 H_2/CO 5 hr at 523°K, spectrum recorded in He at room temperature. (b) 3.3 H_2/CO 6 hr at 523°K, partially hydrogenated in H_2 10 hr at 523°K, spectrum recorded in He at room temperature.

metal is even larger. Again, more than one magnetic field exists and consequently three overlapping sets of six-line components, in addition to one set for residual iron, were used to computer fit this spectrum. The residual metallic iron peaks reveal that carbiding is incomplete even after 6 hr of reaction. This effect of particle size on rate of carbiding will be discussed in more detail later. For this catalyst the computer-fit hyperfine field values of 181, 216, and 116 kOe for the carbide sites are close to those for bulk χ carbide, the monoclinic interstitial alloy of composition Fe_5C_2. The Curie temperature for all three sites of ~505°K, measured by the Mössbauer effect, confirms assignment to the χ phase. This assignment is not completely unambiguous, however, since the asymmetry in the outer peak pairs reveals that the relative spectral areas of the three sites is not equal to the theoretical ratio of $Fe_I:Fe_{II}:Fe_{III} = 2:2:1$, based on the occupation ratio for the three nonequivalent crystallographic locations in χ carbide. Unlike the case for Fig. 1b, this difference cannot be rationalized in terms of coexistence of more than one carbide phase since computer fitting indicated that use of more than three magnetic carbide components was not warranted.

Figure 2 illustrates further the variability of the $Fe_I:Fe_{II}$ ratio on the χ carbide. When the fully carbided catalyst of Fig. 1c was partially hydrogenated in 100 cc/min hydrogen at 523°K for 10 hr, it yielded spectrum b (Fig. 2). Spectrum a (Fig. 2) is for an incompletely carbided catalyst with approximately the same fraction of metallic iron as in b (Fig. 2). The respective spectral parameters, summarized in Table 3, show that the magnitudes of the hyperfine fields are quite comparable, but a significant difference exists in the relative intensities of the χ_I and χ_{II} sites depending on the treatment. These differences are particularly obvious in peak intensities for the outer lines of sites I and II. Changes in the hyperfine field (*23, 24*) and recoil-free fraction (*25, 26*) for surface atoms, nonstoichiometry of the carbide phase, or new transition carbide structures (*20*), could all account for these results.

It should also be noted that some difficulty was encountered in fitting the central portion of the carbided spectrum when the intensities of the individual sets of magnetically split lines were constrained 3:2:1. Two unconstrained peaks added in the final computer fit have near-equal areas. They are taken as a quadrupole-split doublet and assigned to a paramagnetic iron carbide phase on the basis of the isomer shift of +0.25 mm/sec and ΔE_Q in the range 0.8–0.9 mm/sec (*27*). Thus small particle superparamagnetic relaxation effects may be important in considering the relative spectral areas of the different magnetic sites. Mössbauer spectra of bulk χ carbide as a function of temperature, reported by

TABLE 3

Spectral Parameters for Partially Carbided vs Partially Rehydrogenated 10Fe/SiO_2 (Fig. 2)

Treatment	Magnetic site	H (kOe)	Rel. area[a]	IS (mm/sec)
(a) 3.3 H_2/CO 523°K 5 hr	χ-Carbide I	179.5	0.63	+0.24
	II	215.1	0.26	+0.30
	III	108.5	0.11	+0.38
	Fe^0	330.4	—	+0.006
(b) 3.3 H_2/CO 523°K 6 hr	χ-Carbide I	183.5	0.50	+0.21
followed by H_2 523°K	II	216.5	0.36	+0.30
10 hr	III	113.0	0.14	+0.36
	Fe^0	330.7	—	−0.005

[a] Fe^0, free basis.

Maksimov *et al.* (*28*), show that the intensity ratios of the outer hyperfine structure lines for Fe_I and Fe_{II} change, with Fe_I intensity becoming relatively stronger as the Curie temperature is approached.

In summary, we have shown that small iron particles on silica favor formation of ε′ and ε carbide, while larger particles carbide to the χ form during Fischer–Tropsch synthesis at 523°K. These results are interesting in light of the fact that unsupported fused iron catalysts typically form χ carbide at these conditions (*10–12, 29*). Thus, small iron particles favor formation of normally unstable carbides. Not until particle size is increased to around 10 nm does iron approach the behavior of bulk iron catalysts. Dubois and LeCaer (*30*) have shown that several percent of silicon stabilizes ε carbide in bulk iron, and hence we might expect that silica may have an effect on small iron particles.

Additional complexity of the carbide formation is apparent from comparison of our results to those of Amelse *et al.* for 4.94% Fe on Davison silica gel (*13*). The high degree of reduction, relatively small amount of oxidation on exposure to air, appearance of magnetically split α-Fe_2O_3 in the Mössbauer spectra of oxidized samples, and X-ray line broadening measurements of 16 nm for the α-Fe_2O_3 particle size all point to large particles of iron. Yet, when carbided, these particles form the ε′ phase, some of which is superparamagnetic. We can rationalize these results only by assuming that each iron metal particle forms several small, separate grains of carbide. It is interesting to note that the metal particle size is of the order of the pore size of the silica and that strain may play a role in the observed phenomena (*31*).

Effect of Catalyst Support

A 10Fe/MgO precursor was reduced in hydrogen and subsequently treated with 3.3 H_2/CO synthesis gas at 523°K for 6 hr and quenched in He. The Mössbauer spectra of the catalyst precursor, the reduced catalyst, and the carbided catalysts are shown in Fig. 3. The results of the computer analysis are given in Table 4. The spectrum of the precursor reveals that iron is present as Fe^{3+} (*18, 32*). Upon reduction (Fig. 3b) two forms of iron are present; one phase is metallic iron corresponding to the magnetically split component, and the other phase is an irreducible Fe^{2+} phase represented by the central doublet. To obtain a meaningful fit of the data, the position of the hidden inner peak of the magnetic iron was constrained on the basis of the positions of the visible peaks. The dip and width of this peak were also constrained to be equal to the dip and width of the third peak

TABLE 4

Spectral Parameters for 10Fe/MgO (Fig. 3)

Parameters	(a) Precursor	(b) Reduced	(c) Carbided
Magnetic phase	—	Fe^0 330.5	Fe_I 179.3
H (kOe)			Fe_{II} 215.3
			Fe_{III} 113.7
IS (mm/sec)	—	−0.003	Fe_I +0.24
			Fe_{II} +0.30
			Fe_{III} +0.29
Unreduced phase	Fe^{3+}	Fe^{2+}	Fe^{2+}
IS (mm/sec)	+0.34	+1.02	+1.03
ΔE_Q (mm/sec)	0.69	0.70	0.74
Fractional magnetic area	—	0.49	0.50
Fraction of iron in metallic state[a]	0.0	0.49	0.0

[a] Assuming recoil-free fractions of the metal and the oxide are equal.

from the left. This resulted in values of dip and width of the ferrous doublet that were nearly equal. Therefore, in the final fit, equality of dips and widths for these peaks was assumed. Qualitatively, our spectrum is in good agreement with spectra of similar catalysts with different loadings, i.e., 8 and 16% Fe/MgO, investigated by Boudart *et al.* (*18*). Comparison of the results of Shirane *et al.* (*33*) for various (Fe, Mg)O systems, prepared by heating Fe, Fe_2O_3, and MgO in evacuated silica tubes at high temperature, with our data for the Fe^{2+} doublet leads to assignment of this component to Fe^{2+} in the MgO matrix.

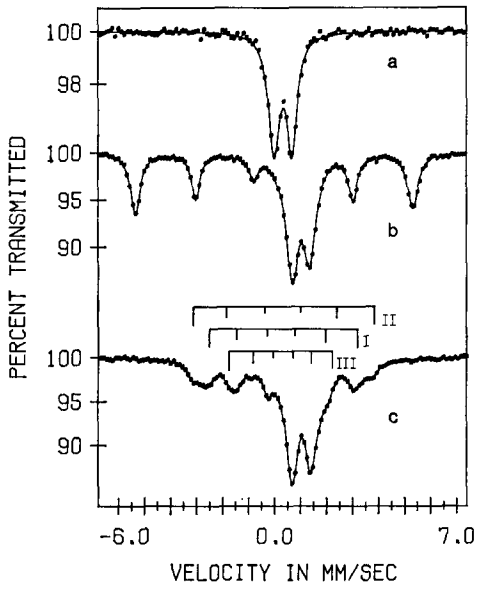

FIG. 3. Mössbauer spectra of 10Fe/MgO. (a) Catalyst precursor recorded *in vacuo* at room temperature; (b) reduced in H_2 12 hr 723°K, recorded in H_2 at room temperature; (c) carbided catalyst after 3.3 H_2/CO 6 hr at 523°K, recorded in He at room temperature. Stick diagrams represent χ carbide.

No metallic iron or iron oxide peaks were evident in the X-ray diffraction pattern of the reduced and passivated sample, confirming that the iron consists of small particles of metal $< \sim 4$ nm in average diameter.

Figure 3c shows that the spectrum of the used 10Fe/MgO catalyst is markedly different from the spectrum of the corresponding reduced catalyst. The computer fit is quite similar to that for the largest particle size 10Fe/SiO_2 sample discussed previously, except for the added complication of the quadrupole split doublet. Specifically, three iron magnetic sites are identified with hyperfine fields nearest those for χ carbide, but with an uncharacteristic site population ratio of Fe_I:Fe_{II}:Fe_{III} = 4.5:2.0:1.0. As before, an additional

constrained central doublet is assigned to a paramagnetic carbide phase on the basis of its isomer shift of +0.28 mm/sec. The discussion of the variability of Fe_I:Fe_{II} ratio presented earlier for the carbided $10Fe/SiO_2$ catalyst also applies to this data.

The carbide assignment to the χ phase means that no carbide stabilization of the kind for small particles of iron on silica occurs for these samples of iron on magnesia. Results on $10Fe/SiO_2$ suggest that smaller iron particles carbide at a faster rate than larger particles. The possibility that observed spectral differences between $10Fe/SiO_2$ and 10Fe/MgO are a result of "reduced time" (reaction time normalized for carbidization rate) differences is ruled out in time-dependent studies presented below. Thus, carbide stabilization on silica must be due primarily to support interaction. Boudart and co-workers (*18*) and Topsøe *et al.* (*34*) conclude that magnesium oxide and iron interact in a manner essential for the ultimate production and stabilization of small metallic particles. Thus, the mere fact that interaction exists between iron metal and the support does not guarantee that a corresponding carbide-stabilizing support interaction also exists.

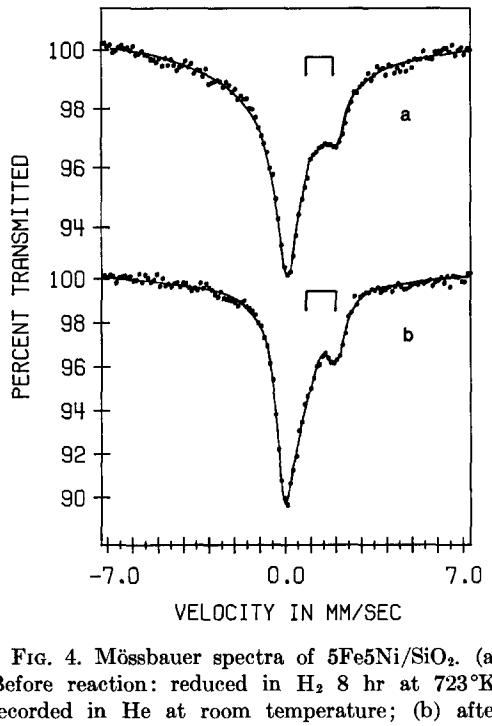

FIG. 4. Mössbauer spectra of $5Fe5Ni/SiO_2$. (a) Before reaction: reduced in H_2 8 hr at 723°K, recorded in He at room temperature; (b) after reaction: 3.3 H_2/CO 6 hr 523°K, recorded in He at room temperature.

TABLE 5

Spectral Parameters for $5Fe5Ni/SiO_2$ (Fig. 4)

Parameter	(a) Reduced	(b) After reaction
FeNi alloy isomer shift (mm/sec)	+0.040	+0.033
FeNi alloy linewidth $\Gamma_{\frac{1}{2}}$ (mm/sec)	1.43	0.957
Fe^{2+} isomer shift (mm/sec)	+1.30	+1.38
Quadrupole split ΔE_Q (mm/sec)	1.04	1.13
Percentage FeNi alloy[a]	65%	63%

[a] Assuming equal recoil-free fractions of the alloy and the oxide.

Effect of Alloying

Synergistic enhancement of activity and selectivity, in addition to increased resistance to poisoning, possible when bimetallic clusters can be formed on a support (*35*), suggest supported alloys as candidates for Fischer–Tropsch synthesis catalysts. Furthermore, one might expect that alloying iron with other Group VIII metals active for Fischer–Tropsch synthesis, such as Co, Ni, or Ru, will change the nature of iron carbide formation during reaction. Nickel and cobalt are known to form unstable carbide phases under certain conditions (*12, 36*); no bulk ruthenium carbide has been documented. In this section we present investigation of the effect of alloying nickel with iron to destabilize carbide formation during reaction.

A reduced $5Fe5Ni/SiO_2$ catalyst was subjected to reaction conditions identical to those for the $10Fe/SiO_2$ and 10Fe/MgO

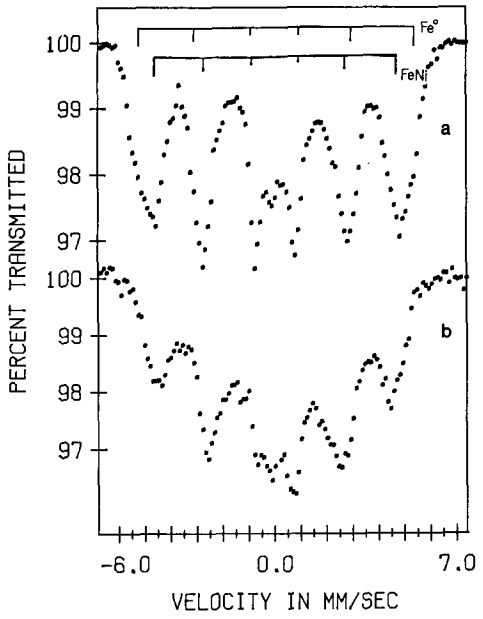

FIG. 5. Mössbauer spectra of phase-separated 5Fe5Ni/SiO_2. (a) Before reaction: reduced in H_2 8 hr at 723°K, recorded in He at room temperature; (b) after reaction: 3.3 H_2/CO 6 hr at 523°K, recorded in He at room temperature.

catalysts and a room temperature Mössbauer spectrum recorded following reaction. The spectra of the catalyst before and after reaction are shown in Figs. 4a and b, respectively. The reduced catalyst consists of iron in two chemical states: a small particle FeNi alloy phase corresponding to the very broad central peak with line-shape characteristic of ferromagnetic particles undergoing superparamagnetic relaxation, and an unreduced ferrous phase indicated by the high velocity shoulder which is the right half of a quadrupole split doublet (*16*).

The spectrum of the used catalyst is qualitatively identical to that for the reduced catalyst. Furthermore, the isomer shift of the paramagnetic FeNi alloy peak has not changed within the limits of experimental error (Table 5). We must conclude, therefore, that no *bulk* FeNi carbide or Fe carbide forms during reaction. The shape of the alloy peak changes noticeably after reaction, however. The peak linewidth narrows from 1.4 to about 1.0 mm/sec indicating an apparent change in the time constant for superparamagnetic relaxation. Since both spectra were recorded at room temperature, the changes in the alloy peak must be attributed to a decrease in particle size, shift in particle size distribution to lower values, and/or an increase in anisotropy energy barrier. The decrease in linewidth is reversible, as shown by a Mössbauer spectrum following a treatment of the spent catalyst in flowing hydrogen at 723°K for 6 hr. Thus, changes due to "redispersion," i.e., particle size decrease accompanying reaction, are unlikely. Reaction conditions, therefore, appear to have increased the anisotropy energy constant. For small (ca. <6 nm) metallic particles, superparamagnetic relaxation may be controlled by surface anisotropy (*19*) which

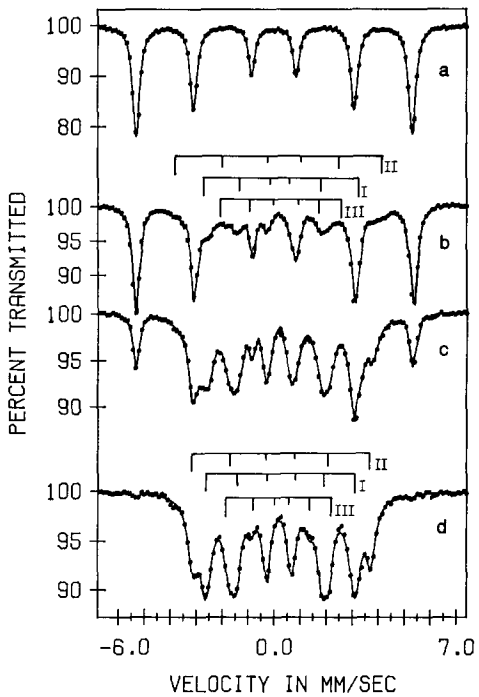

FIG. 6. Reaction time-dependent Mössbauer spectra of 10Fe/SiO_2: (a) t = 0, (b) t = 40 min, (c) t = 180 min, (d) t = 360 min. Reaction conditions: 3.3 H_2/CO, 100 cc/min, 523°K. All spectra recorded in He at room temperature.

can, in turn, be modified by surface reconstruction caused by the reaction gas (*37*). In this case we know only that the particle size is less than d_{cr}, about 10 nm for FeNi (*38*), but we suggest that the observed line narrowing could be a result of surface reconstruction, perhaps due to formation of a surface carbide or graphitic overlayer. Both carbide and graphite surface layers have been seen on Ni single crystals (*39*).

In order to confirm the destabilization of carbide formation in FeNi, we have sought to sinter the particles to sizes greater than the critical diameter (d_{cr}) so that the ferromagnetic splitting at room temperature could be used to aid phase identification. Phase separation accompanying particle growth has frustrated all such attempts (*16*). As shown in Fig. 5, the phase separated $5Fe5Ni/SiO_2$ did carbide during reaction. Accurate computer fits could not be obtained, but subtraction of spectrum a from b (Fig. 5) suggests that the iron-rich phase carbides while the FeNi alloy phase does not.

Catalytically, the $5Fe5Ni/SiO_2$ gave product distributions similar to those of Ni and turnover numbers, based on H_2 adsorption, significantly higher than for Ni (*40*).

Time Dependency of Carbide Formation

The results in the previous sections have shown that a wide variety of iron carbides can be formed on reduced iron catalysts during Fischer–Tropsch synthesis. In addition we conclude that in some cases several carbide phases coexist on an individual catalyst after reaction. These observations, coupled with the knowledge that the metastable $Fe/Fe_xC/C$ system can undergo a variety of solid-phase reactions and transformations, suggest that there may be a time dependency of the carbide phases formed during reaction. To demonstrate this phenomenon, several supported iron catalysts were quenched at intermediate

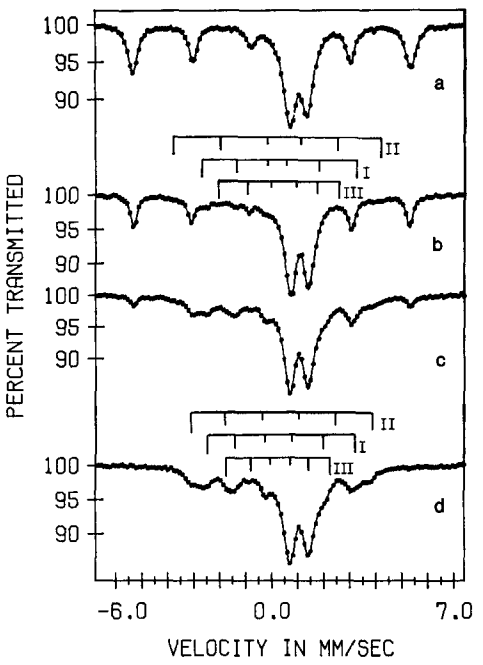

FIG. 7. Reaction time-dependent Mössbauer spectra of 10Fe/MgO: (a) $t = 0$, (b) $t = 4$ min, (c) $t = 40$ min, (d) $t = 360$ min. Reactions conditions: 3.3 H_2/CO, 100 cc/min, 523°K. All spectra recorded in He at room temperature.

reaction times, and room temperature Mössbauer spectra were recorded.

The time dependency of carbide formation during reaction for the large particle $10Fe/SiO_2$ catalyst is represented by the Mössbauer spectra in Fig. 6. The spectrum at time zero shows that the iron is essentially 100% reduced before reaction. After 4 min of reaction there are no detectable changes in the spectrum. Forty minutes of reaction, however, is sufficient time to cause noticeable spectral changes. Although exact curve-fitting of the carbide peaks was difficult due to the large spectral contribution of residual iron, it appears that the carbide phase present after 40 min of reaction is not identical to the carbide phase in the catalyst after the full 6-hr reaction. There is a relatively large carbide contribution with a hyperfine field near 240 kOe, which can only be due to the ϵ(II) carbide site. A computer analysis

TABLE 6

Spectral Parameters for Initial Carbide Formed in 10Fe/SiO_2 and 10Fe/MgO

Parameter		ϵ-carbide Fe_2C (20)	10Fe/SiO_2 t_{rxn} = 40 min	10Fe/MgO t_{rxn} = 4 min
H (kOe)	Fe_I	170 ± 3	172.4	173.6
	Fe_{II}	237 ± 3	241.2	239.0
	Fe_{III}	130 ± 6	136.1	134.1
IS (mm/sec)	Fe_I	+0.20 ± 0.05	+0.25	+0.26
	Fe_{II}	+0.35 ± 0.05	+0.38	+0.36
	Fe_{III}	+0.30 ± 0.05	+0.32	+0.33
Relative area; Fe^0 free basis	Fe_I	0.61	0.59	0.57
	Fe_{II}	0.24	0.28	0.29
	Fe_{III}	0.15	0.13	0.14
H Fe^0		—	331.1	328.5
IS Fe^0		—	+0.002	+0.007
$A_{Fe_xC}/(A_{Fe^0} + A_{Fe_xC})$ Fraction carbided		—	0.42	0.54

with four magnetic components, one for Fe^0 and three for the ϵ carbide, gave an excellent fit both statistically and in agreement with theoretical values for the ϵ phase. Spectral parameters for Fig. 6b are compared with literature values for ϵ carbide in Table 6. After 3 hr of reaction, the iron was approximately 70% carbided and no contribution of ϵ(II) to the Mössbauer spectrum exists. Thus the data indicate that initially an unstable carbide is formed during reaction, and that over a period of time a more stable carbide phase is favored. This general behavior is also followed by the 10Fe/MgO catalyst used in this investigation, with one important difference. Unlike the 10Fe/SiO_2 catalyst which was virtually unchanged after 4 min of reaction, the 10Fe/MgO catalyst was significantly carbided over the same reaction period. The Mössbauer spectra of the 10Fe/MgO catalyst at various stages of reaction are shown in Fig. 7. Again the initial carbide formed is the ϵ phase (see Table 6), but within 40 min the χ phase is the main carbide contribution. Carbiding was complete within 3 hr. It appears from this data that small particles of Fe on SiO_2 and on MgO have reached steady state after 6 hr of reaction at 523°K and, therefore, that the different carbide phases formed do indeed represent an influence of the support.

Similar experiments were run with a 1:1 H_2/CO synthesis gas mixture and reaction temperature of 523°K. The carbide phases formed were identical to those formed with 3.3:1 H_2/CO, but the overall carbiding rate was slightly faster with the equimolar syn-gas mix.

Spectra taken at intermediate reaction times for the intermediate particle size 10Fe/SiO_2 (Fig. 1b), which exhibited simultaneous presence of ϵ' and ϵ carbide, offer further evidence that the carbide found in the used catalyst may not be the same carbide that was formed in the initial stages of reaction. For this catalyst ϵ' carbide formed initially and was partially converted to ϵ carbide as the reaction proceeded. Both phases coexisted after reaction times as long as 12 hr.

The observed differences in carbiding rate between the 10Fe/SiO_2 and 10Fe/MgO catalyst must be due to the significant difference in their respective average metal particles sizes. The strong coupling between carbiding rate and Fischer–Tropsch reaction rate is discussed in the next paper in this series (*17*).

CONCLUSIONS

Using Mössbauer spectroscopy we have observed striking differences in the nature of the iron carbide formed by Fischer–Tropsch synthesis over supported iron catalysts depending on metal particle size, support, and alloying with Ni. These results reiterate the importance of carbide formation when considering the catalytic behavior of iron. Changes in the electronic character of the iron are reflected in the large positive isomer shift values for iron carbide phases. Furthermore, significant structural rearrangement, generally to a much closer packed lattice than bcc α-Fe, accompanies formation of iron–carbon bonds. Structure transformation is easily observed for the ϵ and χ carbides since these phases have three crystallographic positions and hence three magnetically split spectral components; however, the ϵ' and θ phases also have structures quite different from that for metallic iron. The conclusions of this work can be summarized as follows:

(1) The carbide phase formed by iron on silica catalysts during Fischer–Tropsch synthesis is dependent on the average metal particle size; in general, smaller iron particles favor less stable carbides. Some evidence for support-interaction exists.

(2) Alloys roughly equimolar in iron and nickel do not form bulk carbides at our synthesis reaction conditions.

(3) As expected, small iron particles carbide at a significantly faster rate than larger particles.

(4) The initial carbide phase formed in small particles of iron on magnesia and large particles of iron on silica is not the same as the phase observed after long reaction times.

(5) Carbide phases formed at 523°K do not exhibit dependence on the composition of synthesis gas in the range of H_2/CO ratio of 3.3–1.0 though the carbiding rate is slightly increased at low H_2/CO ratio.

ACKNOWLEDGMENTS

We gratefully acknowledge support of this work by NSF (Grant ENG 76-20853) and the NSF Materials Research Program (Grant DMR 76-00889A1). We also thank J. B. Butt and L. H. Schwartz for stimulating discussions and for providing us with a preprint of Ref. (*13*).

REFERENCES

1. Vannice, M. A., *J. Catal.* **37**, 462 (1975).
2. Vannice, M. A., *J. Catal.* **50**, 228 (1977).
3. Garten, R. L., and Ollis, D. F., *J. Catal.* **35**, 232 (1974).
4. Ekerdt, J. G., and Bell, A. T., *ACS Petrol. Div. Preprints* **23**, 475 (1975).
5. Vannice, M. A., and Garten, R. L., *J. Mol. Catal.* 1, 201 (1976).
6. Dalla Betta, R. A., and Shelef, M., *J. Catal.* **48**, 111 (1977).
7. Bond, G. C., and Turnham, B. D., *J. Catal.* **45**, 128 (1976).
8. King, D., *J. Catal.* **51**, 386 (1978).
9. Storch, H. H., Golumbic, H., and Anderson, R. B., "The Fischer–Tropsch and Related Synthesis." Wiley, New York, 1951.
10. Loktev, S. M., Makerenkova, L. I., Slivinskii, E. V., and Ertin, S. D., *Kinet. Katal.* **13**, 1042 (1972).
11. Anderson, R. B., *in* "Catalysis" (P. H. Emmett, Ed.), Vol. IV, pp. 1, 29, 257. Reinhold, New York, 1956.
12. Hofer, L. J. E., *in* "Catalysis" (P. H. Emmett, Ed.), Vol. IV, p. 373. Reinhold, New York, 1956.
13. Amelse, J. A., Butt, J. B., and Schwartz, L. H., *J. Phys. Chem.* **82**, 558 (1978).
14. Schulz, H., and Zein El Deen, A., *Fuel Proc. Tech.* 1, 45 (1977).
15. Ponec, V., *Catal. Rev.-Sci. Eng.* **18**, 151 (1978).
16. Raupp, G. B., and Delgass, W. N., *J. Catal.* **58**, 337 (1979).
17. Raupp, G. B., and Delgass, W. N., *J. Catal.* **58**, 361 (1979).
18. Boudart, M., Delbouille, A., Dumesic, J. A., Khammouma, S., and Topsøe, H., *J. Catal.* **37**, 486 (1975).
19. Boudart, M., Topsøe, H., and Dumesic, J. A., *in* "The Physical Basis for Heterogeneous Catalysis" (E. Dranglis and R. I. Jaffee, Eds.), p. 337. Plenum Press, New York, 1975).

20. Arents, R. A., Maksimov, Yu. V., Suzdalev, I. P., Imshennik, V. K., and Krupyanskii, Yu. F., *Fiz. Metal. Metalloved.* **36**, 277 (1973).
21. Maksimov, Yu. V., Suzdalev, I. P., Arents, R. A., and Loktev, S. M., *Kinet. Katal.* **15**, 1293 (1974).
22. Bernas, H., and Campbell, I. A., *J. Phys. Chem. Solids* **28**, 17 (1967).
23. Shinjo, T., Matsuzana, T., Takada, T., Nasu, S., and Murakami, Y., *J. Phys. Soc. Japan* **35**, 1032 (1973).
24. Van der Kraan, A. M., *Phys. Stat. Sol. (A)* **18**, 215, (1973).
25. Dumesic, J. A., and Topsøe, H., *Adv. Catal.* **26**, 121 (1976).
26. Maradudin, A. A., *Rev. Mod. Phys.* **36**, 417 (1964).
27. Le Caer, G., Simon, A., Lorenzo, A., and Genin, J. M., *Phys. Stat. Sol. (A)* **6**, K97 (1971).
28. Maksimov, Yu. V., Suzdalev, I. P., and Arents, R. A., *Fiz. Tverd. Tela.* **14**, 3344 (1972).
29. Sancier, K. M., Isakson, W. E., and Wise, H., *ACS Petrol. Div. Preprints* **23**, 545 (1978).
30. Dubois, J. M., and Le Caer, G., *Acta Metall.* **25**, 609 (1977).
31. These ideas arose in discussion with L. H. Schwartz, J. A. Amelse, and J. B. Butt.
32. Bhide, V. G., and Tambe, B. R., *J. Mater. Sci.* **4**, 955 (1969).
33. Shirane, G., Cox, D. E., and Ruby, S. L., *Phys. Rev.* **125**, 1158 (1962).
34. Topsøe, H., Dumesic, T. A., Derouane, E. G., Clausen, B. S., Mørup, S., Villadsen, J., and Topsøe, N. Proc. 2nd Int. Symp. on the Scientific Basis for the Preparation and Characterization of Heterogeneous Catalysts, Louvain-la-Neuve, 1978, paper D-3.
35. Sinfelt, J. H., *J. Catal.* **29**, 308 (1973).
36. Goldschmidt, H. J., "Interstitial Alloys," p. 88. Plenum Press, New York, 1967.
37. Dumesic, J. A., Topsøe, H., and Boudart, M., *J. Catal.* **37**, 513 (1975).
38. Suzdalev, I. P., Proceedings of the Conference on the Application of the Mössbauer Effect (Tihany, 1969), p. 193. Akademiai Kiado, Budapest, 1971.
39. Madix, R. J., *Catal. Rev.-Sci. Eng.* **15**, 293 (1977).
40. Lauderback, L. L., Purdue University, unpublished results.